

# Provenance Graph Kernel

David Kohan Marzagão  
 Trung Dong Huynh  
 Ayah Helal  
 Luc Moreau

*Department of Informatics  
 King's College London  
 London, WC2R 2LS, UK*

DAVID.KOHAN@KCL.AC.UK  
 DONG.HUYNH@KCL.AC.UK  
 AYAH.HEHAL@KCL.AC.UK  
 LUC.MOREAU@KCL.AC.UK

## Abstract

Provenance is a record that describes how entities, activities, and agents have influenced a piece of data. Such provenance information is commonly represented in graphs with relevant labels on both their nodes and edges. With the growing adoption of provenance in a wide range of application domains, increasingly, users are confronted with an abundance of graph data, which may prove challenging to analyse. Graph kernels, on the other hand, have been consistently and successfully used to efficiently classify graphs. In this paper, we introduce a novel graph kernel called *provenance kernel*, which is inspired by and tailored for provenance data. It decomposes a provenance graph into tree-patterns rooted at a given node and considers the labels of edges and nodes up to a certain distance from the root. We employ provenance kernels to classify provenance graphs from three application domains. Our evaluation shows that they perform well in terms of classification accuracy and yield competitive results when compared against standard graph kernel methods and the provenance network analytics method while taking significantly less time. Moreover, we illustrate how the provenance types used in provenance kernels help improve the explainability of predictive models.

**Keywords:** kernel methods, data provenance, graph classification, provenance analytics, interpretable machine learning

## 1. Introduction

Similarities between graphs have been often studied in the context graph classification and detection of malicious activity, with a plethora of different methods being proposed to that end (for recent surveys, see Kriege et al., 2020 and Nikolentzos et al., 2019). Such methods explore graph properties using concepts such as shortest paths between nodes (Borgwardt and Kriegel, 2005), sub-trees (Shervashidze et al., 2011; Feragen et al., 2013), or random walks (Gärtner et al., 2003), to mention just a few. In many cases, the graphs being analysed may have continuous or categorical labels for their nodes or edges, but few attention has been given to developing a graph kernel that considers *both* edge and node categorical labels, despite the various graph kernels so far proposed in the literature. A well-known family of graphs that can benefit from such a kernel method is the one of provenance graphs.

Provenance is a form of knowledge graph providing an account of what a system performs, describing the data involved and the processes carried out over those data. More specifically, the World Wide Web Consortium (W3C) defines provenance as a *record that describes the people, institutions, entities, and activities involved in producing, influencing,*

or delivering a piece of data or a thing in the world (Moreau and Missier, 2013). In a provenance graph, inputs/actors and the nature of their influences in such processes are described by labels of its nodes and edges. For instance, the fact that a given entity was generated by a given activity is indicated by an edge labelled *gen* pointing from a node labelled *ent* to another labelled *act*. This simple example illustrates the fact that labels on edges in a provenance graphs starting from a given node can give information about its recent history. If we were to analyse edges positioned further away from a node, we would get a glimpse of the past transformations that are indirectly responsible for its creation.

Provenance is increasingly being captured in a variety of application domains, from scientific workflows (Alper et al., 2013; Chirigati et al., 2013) supporting their reproducibility, to climate science (Ma et al., 2014), and human-agent teams in disaster response (Ramchurn et al., 2016). However, at the same time, users are being confronted with an increasing volume of provenance data, especially from automated systems, making it a challenge to extract meaning and significance from such a deluge. To that end, and inspired by the expressiveness of edge and node labels in provenance graphs conditioned to their distance to a given root node, we introduce a graph kernel method that captures provenance graph patterns efficiently. Our method makes use of the notion of *provenance types*, which places this kernel in the *R*-convolution family of graph kernels (Vishwanathan et al., 2010). Intuitively, provenance types are a simplification of tree-patterns of a given depth  $h$  rooted at a given node. It captures the set of edge-labels occurring at each layer of these tree-patterns, giving an unpolished indication of the node’s past history. Types also take in account the labels of nodes at the leaves of such tree-patterns. For each graph, a feature vector is created: it counts the occurrence of each provenance type encountered in this graph for tree-patterns up to a given depth. We show that the computational complexity of inferring types up to depth  $h$  of nodes in a graph with  $m$  edges is bounded by  $\mathcal{O}(h^2m)$ .

We employ the proposed provenance kernel in classifying provenance graphs in six different data sets from three application domains. We compare the provenance kernel’s accuracy against that of other graph kernels, showing that provenance kernels are competitive in terms of accuracy and at the same time as being fast in terms of execution times. Further, we compare provenance kernels with a provenance-specific graph classification method known as Provenance Network Analytics (PNA) (Huynh et al., 2018). In addition to the theoretical computational complexity, we provide an empirical analysis of the running times of provenance kernels compared against the tested graph kernels and PNA.

Finally, we illustrate how provenance types can provide us with further insights into why a prediction was made. In Section 5, we present an example of how provenance kernels can also be employed by white-box classifications models, i.e. interpretable predictive models where the model provides an explanation for its classification. We discuss the use of white-box models with provenance types and show how they can improve the interpretability of classification tasks.

In summary, the contribution of this paper is threefold:

1. The definition, implementation, and evaluation of a novel graph kernel method, i.e. provenance kernels, that can be applied to graphs with labelled nodes and edges.
2. Provenance kernels are shown to perform competitively in classifying provenance graphs when compared to standard graph kernels and the PNA method.

3. In conjunction with interpretable machine learning (ML) models, provenance types help improve the explainability of classification decisions based on them.

**Paper outline** We first introduce provenance kernels in Section 2, where we provide an algorithm that efficiently infers feature vectors from input graphs to be later used in classification models. Section 3 discusses the related work, as well as provides a comparison of the theoretical computational complexity between provenance kernels and similar models in the literature. Subsequently, in Section 4, we empirically evaluate provenance kernels in six classification tasks in comparison with other established graph kernels and the PNA method. In Section 5, we discuss the use of provenance types in conjunction with interpretable ML models. Finally, we conclude the paper and outline the future work in Section 6.

## 2. Provenance Kernel Framework

In this section, we motivate and present a graph kernel method inspired by particular characteristics of provenance graphs, namely, the chronological aspect represented by relations in such structures. We base our definitions on the PROV data model (Moreau and Missier, 2013), a *de jure* standard for provenance data. We first lay out the provenance foundations and the graph kernel concepts that we will use throughout the paper. We then motivate the idea of provenance types, present the algorithm to infer them, analysing its theoretical computational complexity, to finally provide a formal definition of provenance kernel.

### 2.1 Preliminaries

The main node and edge labels of the PROV framework, as well as their notation to be used throughout this paper, is presented in Table 1. The three node labels shown at the top of the table are called *PROV generic* labels because they are used irrespective of particular provenance applications. The labels of start and destination nodes connected by edges of each given edge label are also specified in, respectively, the third and fourth columns. For a complete description of the PROV data model, refer to Moreau and Missier (2013).

We denote  $G = (V, E, S, L)$  a *provenance graph* in which  $V$  corresponds to the set of nodes of  $G$  with  $|V| = n$ ,  $E$  its set of its directed edges, with  $|E| = m$ . The sets of labels of nodes and edges of  $G$  are denoted, respectively, by  $S$  and  $L$ . An edge  $e \in E$  is a triplet  $e = (v, u, l)$ , where  $v \in V$  is its *starting point*,  $u \in V$  is its *ending point*, and  $l \in L$ , also denoted  $lab(e)$ , is the edge’s *label*.<sup>1</sup> Note that defining edges as triplets instead of pairs allow provenance graphs to have more than one edge between the same pair of vertices. Each node  $v \in V$  can have more than one label, and thus  $lab(v) \in \mathbb{P}(S)$ , where  $\mathbb{P}(S)$  denotes the power-set of  $S$ , i.e., the set of subsets of  $S$ . Note that provenance graphs are *finite*, *directed*, and *multi-graphs* (as there might exist more than one edge between the same pair of nodes).

Considering only PROV generic labels,  $S = \{ag, act, ent\}$ . In case application-specific labels are used, however, set  $S$  is enlarged to also include such specific labels. Regarding edge-labels, typically  $L = \{der, spe, alt, wib, gen, \dots\}$ , where the edge  $(v, u, waw)$ , for example, indicates that activity  $v$  was associated with agent  $u$ . We will often work with more than one graph, and thus we define  $\mathcal{G} = (\mathcal{V}, \mathcal{E}, \mathcal{S}, \mathcal{L})$  as a (finite) family of graphs, in which

---

1. In the absence of ambiguity, we will abuse notation and refer to edges as simply pairs  $(v, u)$

Label	Notation	Source Type	Destination Type
Agent	<i>ag</i>	-	-
Activity	<i>act</i>	-	-
Entity	<i>ent</i>	-	-
wasDerivedFrom	der	<i>ent</i>	<i>ent</i>
specializationOf	spe	<i>ent</i>	<i>ent</i>
alternateOf	alt	<i>ent</i>	<i>ent</i>
wasInvalidatedBy	wib	<i>ent</i>	<i>act</i>
wasGeneratedBy	gen	<i>ent</i>	<i>act</i>
used	use	<i>act</i>	<i>ent</i>
wasAttributedTo	wat	<i>ent</i>	<i>ag</i>
wasAssociatedWith	waw	<i>act</i>	<i>ag</i>
actedOnBehalfOf	abo	<i>ag</i>	<i>ag</i>
wasStartedBy	wsb	<i>act</i>	<i>ent</i>
wasEndedddBy	web	<i>act</i>	<i>ent</i>
wasInformedBy	wifb	<i>act</i>	<i>act</i>

Table 1: PROV generic labels for nodes and edges. The second column shows the notation used for each label throughout this paper. The third and fourth columns show, respectively, the label of source and destination nodes for each edge label. The three first rows represent node labels.

$\mathcal{V}$ ,  $\mathcal{E}$ ,  $\mathcal{S}$ , and  $\mathcal{L}$ , are the union of the sets of, respectively, nodes, edges, node labels, and edge labels of graphs in  $\mathcal{G}$ .

In this work, we will study provenance kernels in both scenarios: when application-specific labels are provided and when they are not. In terms of the generality of graph structures considered in this paper, however, observe that existence of cycles may not be discarded entirely: edges such as usage and generations may create cycles, as well as future invalidation of entities. This is to say that, although edges, for well defined provenance, in general ‘point to the past’, cycles cannot be totally excluded and, for that reason, our definitions will make no restrictive assumptions on graph properties, such as acyclicity. Indeed, the definitions that follow apply to a general graph with labelled edges and nodes.

The *forward-neighbourhood* of a given node  $v \in \mathcal{V}$  is the set of nodes it “points to”, i.e.,  $v^+ = \{u \mid (v, u, l) \in \mathcal{E}\}$ . Analogously, the *backward-neighbourhood* of  $v$  is denoted by  $v^- = \{u \mid (u, v, l) \in \mathcal{E}\}$ . We say a node  $u$  is *distant from*  $v$  by  $x$  if there is a *walk* from  $v$  to  $u$  of length  $x$ , where  $v$  is the walks’s *starting* node, and  $u$  its *ending* node. That is, there is a sequence of  $x$  (not necessarily distinct) consecutive edges starting at  $v$  and ending at  $u$ . More formally, a sequence  $(e_1, \dots, e_s)$  is of consecutive edges iff for  $1 \leq i < s$ , the pair  $e_i = (v_i, u_i, l_i)$  and  $e_{i+1} = (v_{i+1}, u_{i+1}, l_{i+1})$  is such that  $u_i = v_{i+1}$ . The  $x + 1$  nodes in a walk of length  $x$  need not to be distinct. A *path*, on the other hand, is defined as a walk where nodes do not repeat.

A function  $k : \mathcal{X} \times \mathcal{X} \rightarrow \mathbb{R}$  is called a valid *kernel* on set  $\mathcal{X}$  if there is a real Hilbert space  $\mathcal{H}$  and a mapping  $\psi$  such that  $k(x, y) = \langle \psi(x), \psi(y) \rangle$ . In order to show such a Hilbert

space exists (and therefore  $k$  is called its *reproducing kernel*), it is enough to prove that  $k$  is symmetric and positive semi-definite (p.s.d.) (Berlinet and Thomas-Agnan, 2011, Theorem 3), i.e., for every subset  $\{x_1, \dots, x_t\} \subset \mathcal{X}$ , we have that the  $t \times t$  matrix  $M$  defined by  $M(i, j) = k(x_i, x_j)$  is p.s.d. For  $M$  to be p.s.d, we simply need  $\sum_{i,j} c_i c_j M(i, j) \geq 0$  for all  $c_1, \dots, c_t \in \mathbb{R}$ .

## 2.2 Motivation

Consider a node  $v$  in a provenance graph. The set of edges starting at this node may be seen as related to its recent history, i.e., such edges point to other nodes that may, in case of entities, be the activity that generated it, or, in case of activities, be the agent responsible for its execution. Going further, edges that are, in turn, connected to the neighbours of  $v$ , represent  $v$ 's earlier history, and so on. The idea of capturing the label of such edges, as well of nodes, taking in account their distance to the root, lies in the core of what we define as provenance types. Provenance types are the building blocks for provenance kernels.

For example, refer to Fig. 1. It depicts an example of a short patient hospitalisation, from admission to discharging. Here,  $V = \{\text{person13}, \text{patient70}, \text{ward27}, \dots\}$ , while  $S = \{\text{ent}, \text{ag}, \text{act}\}$ . If application-specific types are used,  $S$  is enlarged to include labels such as `mimic:Patient`, `mimic:Ward`, etc. We adopt the standard colour and layout convention for provenance graphs that shows entities as a yellow-filled ellipses, activities as blue-filled rectangles, and agents as orange-filled trapeziums. Time flows downwards in this convention, in which the entities `patient70`,  $\dots$ , `patient73` represent the different 'states' of the same person originally represented by node `person13`, culminating at `patient73` which also contains the provenance-specific label `mimic:DischargedPatient`, indicating that the hospitalisation ended with the discharging of the patient. The activities in this scenario are those that either admit the patient to a ward (`admitting3`) or represent a treatment (`treating5`). Each is associated to the respective hospital ward in which the activity took place.

As a motivation for provenance types, consider nodes `admitting3` and `treating5` in Fig. 1. We can say that they share some similarity as both represent activities in this provenance graph, even though one is an admission and the other a treatment. Further, we can say that they share even more similarities as they are related to entities (via the *use* relation) and to some agent (via the *waw* edge label). Going one step further, however, these nodes do not present the same 'history': `treating5` used an entity which was, in turn, generated by some other activity, whereas `admitting3` did not. We formalise this idea of capturing a simplification of a node's history as the *provenance types* of a node. First, we define label-walks, which will be later used in our definition of types.

**Definition 1 (Label-walk)** Let  $G = (V, E)$  be a directed multigraph. We define a label-walk as

$$LAB(w) = (lab(e_1), lab(e_2), \dots, lab(e_h), lab(u)) \quad (1)$$

where  $w = (e_1, \dots, e_h)$  is a sequence of  $h$  consecutive edges from  $v$  to  $u$ .  $LAB(w)$  is then a sequence of  $h$  edge labels followed by the label of vertex  $u \in V$ . Thus, we say that  $LAB(w)$  is a label-walk of length  $h$ . We further define  $\mathcal{W}^h(v)$  to be the set of all label-walks of length  $h$  starting at a given node  $v$ . In the degenerated case of  $h = 0$ , the start and end nodes coincide and thus  $\mathcal{W}^0(v)$  is defined by simply  $(lab(v))$ .

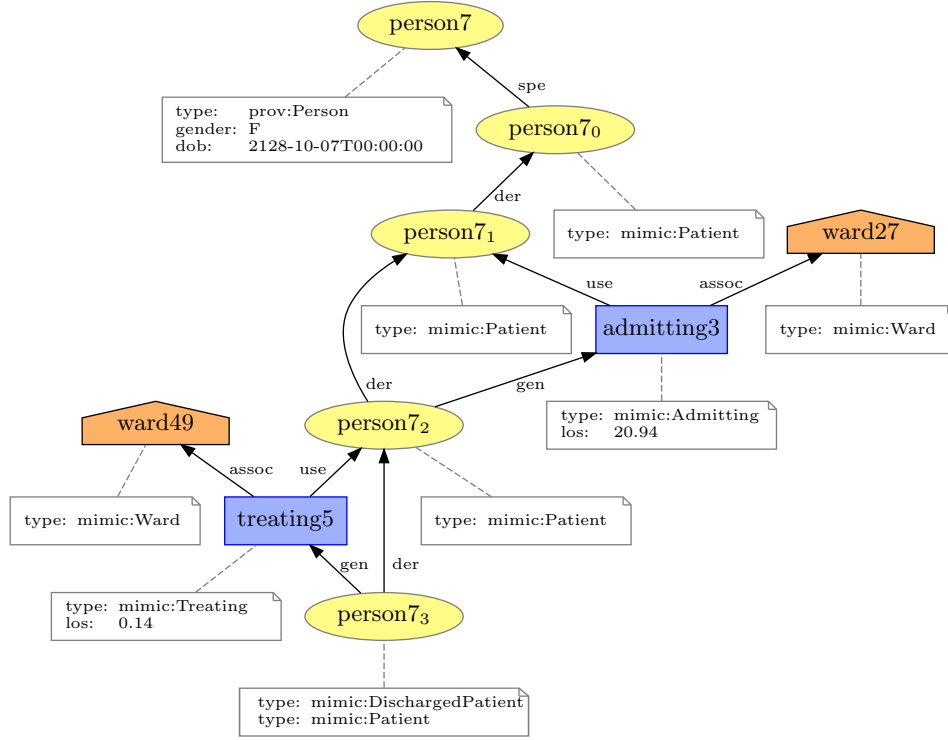


Figure 1: A provenance graph that records the journey of a patient through a hospital admission. Yellow ellipses denote entities, blue rectangles denote activities, and orange trapeziums denote agents. The same patient is recorded multiple times via different entities to represent their different states over time.

In simple terms, a label-walk is the sequence of the labels of edges along a walk followed by the label of its ending node. The intuition behind capturing the label of ending nodes of walks is twofold: first, we are able to define a base case, in which we consider a walk of null size, i.e., capturing only the node's label. Secondly, we are able to make use of application-specific node labels (such as `mimic:Patient`, in Fig. 1), which may provide crucial information for the analysis of provenance data.

**Example 1** *In this example we consider only PROV generic types. Consider the sequence of two consecutive edges given by*

$$w = \left( (patient7_3, treating5, gen), (treating5, patient7_2, use) \right) \quad (2)$$

We have  $LAB(w) = (gen, use, ent)$ . Moreover,

$$\mathcal{W}^2(patient7_3) = \{(gen, use, ent), (gen, waw, ag), (der, der, ent), (der, gen, act)\} \quad (3)$$

We can now define provenance types based on the set of all walks of a given length from each node in  $G$ .

**Definition 2 (Provenance  $h$ -types)** Let  $G$  be a graph and  $v \in V$ . Let  $\mathcal{W}^h(v)$  be the set of all label-walks of length  $h$  starting at  $v$ . We now capture all the labels that are equally distant from  $v$ : we define, for  $1 \leq i \leq h$ ,

$$\tau_i^h = \{\text{lab}(e_{h-i}) \mid (\text{lab}(e_1), \text{lab}(e_2), \dots, \text{lab}(e_h), \text{lab}(u)) \in \mathcal{W}^h(v)\} \quad (4)$$

as the set of edge labels that are in the  $(h-i)$ -th layer when counting from  $v$ .<sup>2</sup> For  $i = 0$ , we define

$$\tau_0^h = \{\text{lab}(u) \mid (\text{lab}(e_1), \text{lab}(e_2), \dots, \text{lab}(e_h), \text{lab}(u)) \in \mathcal{W}^h(v)\} \quad (5)$$

We say that the provenance  $h$ -type of  $v$  is a sequence of sets given by

$$\phi^h(v) = (\tau_h^h, \dots, \tau_0^h) \quad (6)$$

In the case  $\mathcal{W}^h(v) = \emptyset$ , i.e. there is no walk of length  $h$  from  $v$ , we define  $\phi^h(v) = \emptyset$ . When clear from the context, we shall denote  $\tau_i^h(v)$  as simply  $\tau_i(v)$ , or even  $\tau_i$ .

**Example 2** Consider node *patient73* discussed in Example 1. Its 2-type combines the label-walks from Equation 3 to generate:

$$\phi^2(\text{patient73}) = (\underbrace{\{\text{gen}, \text{der}\}}_{\tau_2^2}, \underbrace{\{\text{use}, \text{waw}, \text{der}, \text{gen}\}}_{\tau_1^2}, \underbrace{\{\text{ag}, \text{act}, \text{ent}\}}_{\tau_0^2}) \quad (7)$$

Further, consider nodes *admitting3* and *treating5* once again in Fig. 1. Their 0-types, 1-types, and 2-types are given by:

$$\begin{aligned} \phi^0(\text{admitting3}) &= \phi^0(\text{treating5}) = (\{\text{act}\}) \\ \phi^1(\text{admitting3}) &= \phi^1(\text{treating5}) = (\{\text{assoc}, \text{use}\}, \{\text{act}, \text{ag}\}) \\ \phi^2(\text{admitting3}) &= (\{\text{use}\}, \{\text{der}\}, \{\text{ent}\}) \\ \phi^2(\text{treating5}) &= (\{\text{use}\}, \{\text{der}, \text{gen}\}, \{\text{act}, \text{ent}\}) \end{aligned}$$

These were both examples using only PROV generic types. By using application-specific types for the same two nodes *admitting3* and *treating5*, on the other hand, we have

$$(\{\text{act}, \text{mimic:Admitting}\}) = \phi^0(\text{admitting3}) \neq \phi^0(\text{treating5}) = (\{\text{act}, \text{mimic:Treating}\}) \quad (8)$$

Note that two different sets of label-walks may give rise to the same provenance type, although the converse is not true, i.e., two different types cannot come from the same set of label-walks. This implies that the function that maps sets of label-walks to types is not, in general, injective. We claim that this is beneficial as it unifies different sets of label-walks that have very similar meaning in provenance. Note also that multiple occurrences of the same walks starting at  $v$  carry out no difference in  $v$ 's provenance types as opposed to just one copy of each different walk.

---

2. This apparent reversed choice of indexing will simplify the algorithm to infer such provenance types presented in the next section. The intuition is that, with this notation,  $\tau_0^h$  always refers to node labels for any  $h$ .

Algorithm 1: INFERRING TYPES UP TO  $h$  ( $\mathcal{V}, \mathcal{E}, h$ )

---

```

1  initialise for all  $v \in \mathcal{V}$  and for all  $i \leq h$ 
2       $\phi^i(v) \leftarrow \emptyset$ 
3      for all  $0 \leq j \leq i$ ,  $\tau_j^i(v) \leftarrow \emptyset$ 
4  for  $v \in \mathcal{V}$ 
5       $\tau_0^0(v) \leftarrow \text{lab}(v)$ 
6       $\phi^0(v) \leftarrow (\tau_0^0(v))$ 
7  for  $1 \leq i \leq h$ 
8      for each edge  $e = (v, u) \in \mathcal{E}$  such that  $\phi^{i-1}(u) \neq \emptyset$ 
9          add  $\text{lab}(e)$  to  $\tau_i^i(v)$ 
10     for  $0 \leq j \leq i-1$ 
11          $\tau_j^i(v) \leftarrow \tau_j^i(v) \cup \tau_j^{i-1}(u)$ 
12      $\phi^i(v) \leftarrow (\tau_h^i(v), \dots, \tau_0^i(v))$ 
13 return  $\phi^i(v)$  for all  $v \in \mathcal{V}$  and  $0 \leq i \leq k$ 

```

---

Figure 2: An algorithm that receives nodes and edges of a family of graphs, a parameter  $h$ , and outputs all provenance types  $\phi^0(v), \dots, \phi^h(v)$  for all nodes  $v$ .

### 2.3 Algorithm

We now present an algorithm that infers all  $\phi^i$  for  $0 \leq i \leq h$  for nodes in a family of graphs  $\mathcal{G}$  in  $O(h^2M)$ , where  $M$  is the total number edges among graphs in  $\mathcal{G}$ . For a single graph, the algorithm runs in  $O(h^2m)$ , where  $m$  is the number of edges in this particular graph.

#### 2.3.1 THE ALGORITHM

Fig. 2 provides an algorithm to infer provenance  $h$ -types. First, we initialise all types  $\phi^i(v)$  with the empty set for all depths up to  $h$  and all nodes. Moreover, we initialise as empty sets the building blocks of our  $h$ -types that record the labels of edges seen in at a given distance from each node (lines 1-3). The intuition behind this explicit initialisation is that if we do not update a given  $\phi^i(v)$ , the empty set will indicate that there are no label-walks of size  $i$  starting at  $v$ . This will be used later as a condition in line 8.

The loop starting at line 4 infers the base of our algorithm: the 0-type of all nodes, i.e.,  $\phi^0(v)$ , which is simply the set of labels of  $v$  for each  $v \in \mathcal{V}$ .

Each iteration of the loop starting in line 7 will infer the  $i$ -type for all nodes. We first loop through all edges in  $\mathcal{E}$  that can ‘lead us somewhere’. In other words, we are considering only edges  $e = (v, u)$  that belong to walks of size  $i$  starting at  $v$ . This is true if and only if  $\phi^{i-1}(u) \neq \emptyset$ . We then make sure that label of  $e$  is added to the set  $\tau_i^i(v)$  (line 9).

Finally, the loop starting at line 10 adds to the set of  $\tau_j^i(v)$  the labels from set  $\tau_j^{i-1}(u)$ . We can finally in line 12 construct the entire  $i$ -type for all nodes.

To see that the algorithm correctly infers provenance types, note that line 8 guarantees that all label-walks of length  $i$  starting at  $v$  will be identified. Further, that lines 10 and 11 make sure that all labels in each of these label-walks will be fully inspected and added to  $v$ ’s type accordingly.



### 2.3.2 COMPLEXITY ANALYSIS

We are now showing that we need  $O(h^2M)$  operations to infer the  $\phi^h(v)$  for each node  $v$  in a family of graphs  $G_1, \dots, G_s := \mathcal{G}$ . Here,  $N$  stands for the sum of the number of nodes in all provenance graphs and  $M$  for the sum of the number of edges. Similarly to the evaluation of Weisfeiler-Lehman graph kernels in Shervashidze et al. (2011), we can infer the types of nodes on each graph in parallel. Lines 1-3 can be done in  $O(h^2N)$ , since we are initialising  $\frac{1}{2}(h+1)(h+2)$  sets for each node in  $\mathcal{V}$ . Lines 4-6 take  $O(N)$ . Let us now investigate the *for* loop initiated in line 7. We are entering this loop  $h$  times, and in each of them we are investigating each edge at most once (loop stating in line 8), and finally, for each edge, we are performing at most  $h$  pairwise operations on sets of constant size (bounded by  $\max\{|T|, |L|\}$ ). Line 12 takes  $O(N)$ . Thus loop starting at line 7 can be done in  $O(h^2M)$ , assuming  $N = O(M)$ . Which gives us the overall running time bounded by  $O(h^2M)$  when we assume  $N = O(M)$ .

### 2.4 Provenance Kernel

In this section, we define the mapping of graphs into a high dimensional space by simply counting the number of occurrences of each provenance  $h$ -types up to depth  $h$ . We formally define a feature vector in the following definition.

**Definition 3 (Feature Vector)** *Let  $\mathcal{G}$  be a family of graphs and define  $\phi^h(\mathcal{V}) = \{F_1, \dots, F_s\}$  as the (enumerated) set of all provenance types of depth **up to**  $h$  encountered in  $\mathcal{V}$ . The feature vector of a graph  $G \in \mathcal{G}$  is given by:*

$$VEC^h(G) = (x_1, x_2, \dots, x_s) \quad (9)$$

where  $x_i = |\{v \mid \phi^h(v) = F_i, \text{ and } v \in G\}|$

Note that Definition 3 explicitly considers the possibility parallel inference of feature vectors among all graphs in a family  $\mathcal{G}$ , as suggested by Shervashidze et al. (2011) in the context of of the number of edges, similarly to the evaluation of Weisfeiler-Lehman graph kernels. In fact, this property comes from the fact that provenance kernels are an explicit graph kernel, i.e., the feature vectors, and not only the dot products between each pair, are known (for other examples of explicit graph kernels, see Nikolentzos et al. 2019, p. 14). We apply this definition to our graph in Fig. 1 as an example.

**Example 3** *Consider the provenance graph  $G$  depicted in Fig. 1. In order to infer  $VEC^1(G)$ , we need  $G$ 's 0-types and 1-types. There are three of the former and four of the latter, and we denote them by:*

$$\begin{aligned} F_1 &= (\{act\}) & F_2 &= (\{ag\}) & F_3 &= (\{ent\}) \\ F_4 &= (\{waw, use\}, \{act, ag\}) & F_5 &= (\{spe\}, \{ent\}) & F_6 &= (\{der\}, \{ent\}) \\ F_7 &= (\{gen, der\}, \{act, ent\}) \end{aligned}$$

And thus

$$VEC^1(G) = (5, 2, 2, 2, 1, 1, 2) \quad (10)$$

We now use the definition of a feature vector to define provenance kernels.

**Definition 4 (Provenance Kernel)** *Given two graphs  $G, G' \in \mathcal{G}$  and  $\phi^i(\mathcal{V})$  for all  $0 \leq s \leq h$ , we define the kernel between  $G$  and  $G'$  as*

$$k^h(G, G') = \sum_{s=0}^h \langle \text{VEC}^s(G), \text{VEC}^s(G') \rangle \quad (11)$$

where  $\langle x, y \rangle$  denotes the dot product between  $x$  and  $y$ .

**Proposition 5** *Provenance kernels are p.s.d.*

**Proof** Let  $c_1, \dots, c_t \in \mathbb{R}$  and  $G_1, \dots, G_t \in \mathcal{G}$ . Consider for a given depth  $s$  and pair of indices  $i, j$ , the dot product  $\langle \text{VEC}^s(G_i), \text{VEC}^s(G_j) \rangle$ . Then,

$$\sum_{i=1}^t \sum_{j=1}^t c_i c_j \langle \text{VEC}^s(G_i), \text{VEC}^s(G_j) \rangle = \langle \sum_{i=1}^t c_i \text{VEC}^s(G_i), \sum_{j=1}^t c_j \text{VEC}^s(G_j) \rangle \geq 0 \quad (12)$$

The inequality follows from the fact that both sums add to exactly the same value and from  $\langle x, x \rangle \geq 0$  for all  $x$ . Since sum of non-negative numbers is non-negative,  $k^h$  is p.s.d.  $\blacksquare$

In the next section, we propose a metric over provenance  $h$ -types, with which it is possible to analyse how similar two nodes are with respect to their types. This comparison can be done between nodes from same or different graphs.

## 2.5 A Natural Metric over Provenance Types

Provenance types as defined in Definition 2 give rise to a well defined metric over the set of all types. By looking at sets  $(\tau_h, \dots, \tau_1, \tau_0)$  in  $\phi^h(v)$  and  $\phi^h(u)$  we may be able to tell how distant a pair of corresponding sets are by, for example, their Hamming distance. Given two sets  $A$  and  $B$ , the Hamming distance  $m(A, B)$  is the number of elements in which  $A$  and  $B$  differ, i.e.,

$$|(A \cup B) \setminus (A \cap B)| \quad (13)$$

We abuse notation and extend this definition to full types by adding the Hamming distance of each of the nodes or edge label sets and later normalising it by the sum of all different labels seen in each level as follows:

$$m(\phi^h(v), \phi^h(u)) = \frac{\sum_{i=0}^h m(\tau_i(v), \tau_i(u))}{\sum_{i=0}^h |\tau_i(v) \cup \tau_i(u)|} \quad (14)$$

Note that, instead of normalising each level, we do so at the end, after adding all the distances up to  $h$ . Therefore, the normalised Hamming distance of two provenance types ranges from 0 to 1, the former representing types are identical, whereas the latter indicates there is no single common label at the same depth between two types.

**Example 4** Recall the 2-types of nodes *admitting3* and *treating5* (with only application-agnostic node types) discussed in Example 2:

$$\begin{aligned}\phi^2(\textit{admitting3}) &= (\{use\}, \{der\}, \{ent\}) \\ \phi^2(\textit{treating5}) &= (\{use\}, \{der, gen\}, \{act, ent\})\end{aligned}$$

Their Hamming distance is given by:  $m(\phi^2(\textit{admitting3}), \phi^2(\textit{treating5})) = \frac{2}{5}$ .

Finally, we introduce the notion of a type being an *extension* of another provenance type. This allow us to compare types of different depths. Formally, for  $h > h'$ , we say that  $v$ 's type  $\phi^h(v)$  is an extension of  $u$ 's type  $\phi^{h'}(u)$  if, and only if,  $\tau_i(u) = \tau(v)$  for all  $i = 0, \dots, h'$ . Taking Fig. 1 once more as an example, we can say that  $\phi^2(\textit{patient7}_1) = (\{der\}, \{spe\}, \{ent\})$  is an extension of  $\phi^1(\textit{patient7}_0) = (\{spe\}, \{ent\})$ .

With a well defined distance over the set of our graph kernel features, we are able to define a new graph in which nodes are provenance types, and edges correspond to their Hamming distance. With that, we are able to infer analogous graph properties such as width, average distance, average cluster coefficient (Kalna and Higham, 2006). We leave for future work the analysis of the relevance of such metrics on classification algorithms.

### 3. Related Work

Similar definitions of provenance types have been proposed as a tool for provenance graph summarisation (Moreau, 2015; Kohan Marzagão et al., 2020). In both these approaches, the idea of the history of provenance nodes being related to a sequence of transformations described by edge labels is used. To the best of our knowledge, however, this is the first work to explore the use of provenance types in the context of machine learning methods. When comparing the efficiency of the other summarisation methods with our own, we find that the definition by Moreau (2015) requires an exponential time  $\mathcal{O}(nd^h)$ , where  $d$  is the maximum degree of nodes in an input graphs, and  $n$  its number of nodes. On the other hand, Kohan Marzagão et al. (2020) propose a faster algorithm that takes  $\mathcal{O}(hm)$ , where  $m$  is the number of edges of an input graph. This is faster than our algorithm by a factor of  $h$ , which is typically small and does not depend on the size of the graph. This faster algorithm, however, shares similarities with Weisfeiler-Lehman graph kernels to a point in which patterns with very close meaning in provenance are classified differently. More specifically, the algorithm does not inspect sub-trees beyond their first level in order to discard repetitions. This is discussed in detail later in this section and exemplified in Fig. 3.

ML techniques on graphs have been proposed in the domain on provenance. Provenance Network Analytics (PNA) (Huynh et al., 2018), for example, creates, for each graph, a feature vector that encodes a sequence of different graph topological properties. Some of these are provenance agnostic, such as the number of nodes, or the number of edges. Others, in contrast, record the longest shortest paths between two provenance entities, or between an agent and an activity, for instance. In Section 4, we compare the performance of provenance kernels and PNA in the same classification tasks.

Provenance kernels compare and classify graphs, as opposed to comparing and classifying nodes on graphs. The latter is often known as kernels *on graphs* (as opposed to *graph kernels*), or *graph embedding* techniques. A notable example of graph embedding technique

is Struc2Vec (Ribeiro et al., 2017) is a learning technique based on the structural identity of nodes on graphs that embed nodes into a Euclidean space according to the structure of their neighbourhood. Similarly to provenance kernels, struc2vec has a hierarchical approach when looking at the structure of the neighbourhood of nodes. The main difference to our work is that Struc2Vec does not consider edge nor node labels, but instead the number of occurrences of neighbouring elements (and their degrees). Another commonality is that both works define a distance between nodes based on their neighbours and a suitable metric. In the context of knowledge graphs, graph embedding for link prediction was used in Rosso et al. (2020). ML methods for Resource Description Framework (RDF) graphs have been studied by L  sch et al. (2012) and De Vries and De Rooij (2015). The former work used implicit computations to compare a pair of graphs, whether the latter introduced explicit methods allowing for faster computation (for a survey on similar models, see Ristoski and Paulheim 2016). Other known approaches that for example aim to find missing labels or links in graphs are NodeSketch (Yang et al., 2019), DeepWalk (Perozzi et al., 2014), and Node2Vec (Grover and Leskovec, 2016).

Among of the graph kernel methods proposed in recent years, Weisfeiler-Lehman (WL) graph kernels share the most commonalities with provenance kernels. Most notably, provenance kernels can be seen as belonging to the WL framework: a sequence of labelled graphs  $G_1, \dots, G_h$  is generated iteratively by updating node labels each time. Both are R-convolution kernels (Vishwanathan et al., 2010) since graphs are first partitioned (each partition being a node) and their parts are then compared. Also, both take into account patterns around nodes with a given depth  $h$  using an inductive algorithm that only takes into account smaller patterns of neighbouring nodes. On the other hand, the WL graph kernel algorithm presented by Shervashidze et al. (2011) does not consider edge labels. A possible extension for labelled edges, however, is mentioned in their original work and made explicit by de Vries (2013). A close variant to this extension was also proposed by Kohan Marzag  o et al. (2020), with the differences that (1) repetitions of branches from the same given parent in its walk-tree are discarded and; (2) although all edge-labels were considered, only nodes at the leaves of trees had their labels taken in account. Discarding repetitions is key in reducing the sizes of feature vectors by putting together patterns that have a similar meaning in provenance. In this paper, we extend this process further by agglutinating even more similar patterns into the same provenance type. Fig. 3 shows two examples of such types. In essence, the extra sequence of two derivations in Pattern 1 does not add qualitative meaning to the set of transformations that lead to the creation of the root node. Provenance kernels, on the other hand, consider these two patterns as having the same type. It is possible to see provenance types for provenance kernels as a *flattened* version of the ones defined by Kohan Marzag  o et al. (2020) since the idea of branches is hidden by the sole enumeration of labels at a given depth.

In terms of theoretical computational complexity, provenance kernels are situated in the efficient spectrum. Note that provenance kernel’s computational complexity for one graph with  $m$  edges,  $\mathcal{O}(h^2m)$ , is bounded by  $\mathcal{O}(h^2nd)$ , where  $d$  is the maximum (out) degree and  $n$  is the number of nodes of this graph. Also,  $m = nd$  if and only if the input graph is regular. Graphlet Sampling kernel (GS) (Pr  zulj, 2007) counts the number of small subgraphs present in each input graph. These small subgraphs typically have size  $k \in \{3, 4, 5\}$ . The original time required to run this kernel,  $\mathcal{O}(n^k)$ , is prohibitively expensive. Later, Shervashidze et al.

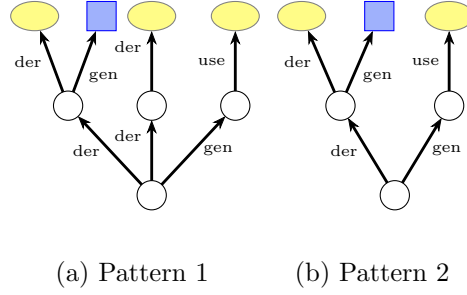


Figure 3: Two examples of different tree-patterns that have a similar meaning in provenance. Yellow circles denote entities, blue squares denote activities, and plain circles denote nodes of which types are not captured by the algorithm. Provenance kernels classify both these tree-patterns as the same 2-type, i.e.,  $(\{der, gen\}, \{der, gen, use\}, \{act, ent\})$ .

(2009) improved this bound to  $\mathcal{O}(nd^{k-1})$ , where  $d$  is the maximum degree of nodes in an input graph. Neighbourhood Hash kernel (NH) (Hido and Kashima, 2009) compares graphs by counting the number of common node labels, which are updated with the employment of logical operations that take in account the label of neighbouring nodes. These operations do not use the original categorical node label, but a binary array so XOR operations can be employed. The complexity of this kernel is bounded by  $\mathcal{O}(bhn\bar{D})$ , where  $\bar{D}$  is the average degree of the vertices,  $h$  is how many times the update is executed, and  $b$  is the number of bit labels. We need  $2^b - 1 \gg |\Sigma|$ , size of the label set. Finally, Neighborhood Subgraph Pairwise Distance kernel (NSPD) (Costa and De Grave, 2010) compares subgraphs  $S$  in the neighbourhood of nodes up to a distance  $r$  for all pair of nodes in a given graph. The complexity,  $\mathcal{O}(n|S||E(S)|\log|E(S)|)$ , is such that  $S$  is the subgraph induced by the neighbourhood of a vertex and radius  $r$ .  $E(S)$  is the number of edges of  $S$ .

We can see that some of the theoretical gaps on running times between provenance kernels and the others discussed above come down to low-impact variables that may even be treated as constants, such as the number of bit labels or the size of graphlets. Others, such as maximum degrees and number of edges of neighbourhood subgraphs, are more dependent on input graphs and tend to have more impact on running times, which indicate that provenance kernels are computed faster. These differences are reflected in the empirical running times evaluated in Section 4, in which we show that provenance kernels outperform the three methods described above (GS, NH, and NSPD) in terms of efficiency. Moreover, none of these is designed to take as input the edge categorical labels of graphs. Subgraph Matching kernel, on the other hand, does consider both edge and node labels as it counts the number of common subgraphs of bounded size  $k$  between two graphs. It requires, however, an impractical computational running time of  $\mathcal{O}(kn^{k-1})$ , where  $n$  this time stands for the sum of sizes of the two graphs being compared. In fact, this kernel timed out in our experiments and its accuracy could not be measured.

Table 2 presents a summary of all graph kernels to be compared to provenance kernels in Section 4. In this table, we note whether node or edge categorical labels were taken into account in the implementation we used, as well as their theoretical complexity. We now briefly discuss the remaining kernel methods. The Shortest Path kernel (SP) (Borgwardt and Kriegel, 2005), for each graph, constructs a new graph that captures the original graph’s

Table 2: The graph kernels evaluated in Section 4 and their properties: whether node and edge categorical labels are considered and their theoretical computational complexity.

Kernel Method	Node label	Edge label	Complexity
Provenance Kernels (PK)	✓	✓	$\mathcal{O}(h^2m)$
Shortest Path (SP)	-	-	$\mathcal{O}(n^4)$
Vertex Histogram (VH)	✓	-	$\mathcal{O}(n)$
Edge Histogram (EH)	-	✓	$\mathcal{O}(m)$
Graphlet Sampling (GS)	-	-	$\mathcal{O}(nd^{k-1})$
Hadamard Code (HC)	✓	-	$\mathcal{O}(bhn\bar{D})$
Weisfeiler-Lehman (WL)	✓	-	$\mathcal{O}(hm)$
Neighbourhood Hash (NH)	✓	-	$\mathcal{O}(bhn\bar{D})$
Neigh. Subgraph P. Dist. (NSPD)	-	-	$\mathcal{O}(n S  E(S)  \log  E(S) )$

shortest paths and then uses a base kernel to compare two shortest path graph’s. The complexity of SP is  $\mathcal{O}(n^4)$ . We use the algorithm of Vertex Histogram (VH) and Edge Histogram (EH) kernels as presented by Sugiyama and Borgwardt (2015). VH creates, for each graph, a feature vector that captures the number of nodes with each given node label  $l$ , whereas EH does the analogous for edge labels. Their computational complexities are  $\mathcal{O}(n)$  for VH and  $\mathcal{O}(m)$  for EH. Note that provenance kernels of depth 0 coincide with VH. Hadamard Code kernel (HC) (Kataoka and Inokuchi, 2016) is similar to NH, even by showing the same computational complexity. It explores the neighbourhood of nodes iteratively for different levels (or depths). Its name come from the use of Hadarmard code matrices.

Finally, when compared against the PNA method, provenance kernels outperform in terms of theoretical computational complexity. One of the features considered in the PNA method is the longest shortest path between two nodes of a given label (two entities, or one entity and one activity, and so on). This gives us a lower bound for PNA’s computational complexity of  $\Omega(nm)$ .

The next section reports the results of our empirical evaluation of provenance kernels over classification tasks in three different application domains, in which we also investigate the impact of including application-specific labels as opposed to only considering application-agnostic ones in each learning task.

## 4. Empirical Evaluation

As a tool for analysing provenance graphs, provenance kernels are suitable for ML techniques over provenance data. In order to demonstrate the approach, we test provenance kernels in a number of classification tasks on six provenance data sets (described in the following section). In our evaluation, we compare the accuracy of provenance kernels against generic graph kernels and the PNA method (discussed in Section 3) in the same classification tasks. We describe the evaluation methodology in Section 4.2 and report the evaluation’s results in Section 4.3.

## 4.1 Data sets

We employed six provenance data sets in our evaluation; they were produced by three different applications: MIMIC (Johnson et al., 2016), CollabMap Ramchurn et al. (2013), and a Pokémon Go simulator. These applications cover a spectrum of human and computational processes. The first, MIMIC, records solely human activity; the second, CollabMap, is created with computational workflows driven by human inputs, whereas Pokémon Go is a fully synthetic system. We now provide an overview of these applications.

### 4.1.1 MIMIC APPLICATION

MIMIC-III (Johnson et al., 2016) is an openly available data set comprising de-identified health data associated with over 53,000 intensive care unit admissions at a hospital in the United States. It contains details collected from hospital stays of over 30,000 patients, including their vital signs and medical measurements, the procedures done on them and by whom, their diagnostics, etc. In this application, we use the data from MIMIC-III to reconstruct a patient’s journey through the hospital in a provenance graph (see Fig. 1 for an example). Each admission starts with the patient being admitted at a hospital ward or unit and followed by transfers from one unit to another. The patient before and after a stay in the care of a ward/unit are modelled as two separate entities in the provenance graph, the latter derives from the former as a result of the corresponding ‘treatment’ activity associated with the respective ward/unit. In addition, each *procedure* (e.g. inserting peripheral lines, imaging, ventilation) that was carried out on the patient is similarly modelled as an activity with two entities to represent the patient before and after the procedure. Both types of activities can happen in parallel. We also annotate procedure activities with their procedure types, e.g. `process:225469`, specifying what the procedures are. There are 116 different types of procedures recorded in the data set; out of those, 8 types are in the “Communication” category, e.g. meeting the family, notifying the family. Since those do not clinically affect a patient, we ignore them in our analyses, leaving 108 procedure types recorded in the provenance graphs we produced.

Approximately 10% of the data set’s admissions resulted in in-hospital mortality. For each hospital admission, we associate its provenance graph with a `dead` label, which has either a value of 0 or 1, with 1 representing in-hospital mortality. We then aim to predict the mortality result from a patient’s journey during admission by applying the provenance kernels over its provenance graphs. This set of provenance graphs is now called MIMIC.

### 4.1.2 COLLABMAP APPLICATION

CollabMap (Ramchurn et al., 2013) is a crowdsourcing platform for constructing evacuation maps for urban areas. In these maps, evacuation routes connect exit of buildings to the nearby road network. Such routes need to avoid obstacles that are not explicit in existing maps (e.g. walls or fences). The application crowdsources the drawing of such evacuation routes from the public by providing them aerial imagery and ground-level panoramic views of an interested area. It allows non-experts to perform tasks without them needing expertise other than drawing lines on an image. The task of identifying all evacuation routes for a building was broken into micro-tasks performed by different contributors: building identification (outline a *building*), building verification (vote for the building’s correctness),

route identification (draw an evacuation *route*), route verification (vote for the correctness of routes), and completion verification (vote on the completeness of the current *route set*). This setup allows individual contributors to verify each other’s contributions (i.e. buildings, routes, and route sets).

In order to support auditing the quality of its data, the provenance of crowd activities in CollabMap was fully recorded: the data entities that were shown to users in each micro-task, the new entities generated afterwards, and their dependencies. The provenance graphs from CollabMap are, therefore, recorded the actual activities as they occurred and are not reproduced after the fact. More details on CollabMap provenance graphs are provided by Huynh et al. (2018). A notable point of this data set is that the provenance graph associated with a data entity does not describe its history but the later entities and activities that depended on it. Hence, given an entity, such a graph was called a (provenance) *dependency graph* of that entity (Huynh et al., 2018), which is analogous to a graph detailing the citations of an academic paper, their later citations, and so on. More formally, the dependency graph of a node  $v$  in a provenance graph  $G$  is the sub-graph of  $G$  induced by all nodes from which it is possible to reach  $v$ , i.e., the sub-graph induced by the set of nodes  $S = \{u \mid \text{there exists a walk from } u \text{ to } v\}$ .

In 2012, CollabMap was deployed to help map the area around the Fawley Oil refinery in the United Kingdom. It generated descriptions for 5,175 buildings, 4,997 routes, and 4,710 route sets. In this application, we aim to predict the quality of CollabMap data entities from their provenance dependency graphs, i.e. whether a building, route, or route set is sufficiently trustworthy to be included in the final evacuation map. The sets of provenance dependency graphs for CollabMap buildings, routes, and route sets are provided by Huynh et al. (2018) along with their corresponding `trusted` or `uncertain` labels; they are named as CM-B, CM-R, and CM-RS, respectively.

#### 4.1.3 POKÉMON GO SIMULATOR

Pokémon Go is a location-based augmented reality mobile game in which players, via a mobile app, search, capture, and collect Pokémon that virtually spawn at geo-locations around them (Paavilainen et al., 2017). In this application, we simulated part of the game’s mechanics using NetLogo (Tisue and Wilensky, 2004), a multi-agent programmable modelling environment. It supports the concept of mobile *turtles* on a square grid of stationary *patches*. Each turtle, therefore, is located on a patch, essentially a 2-dimensional coordinate. The turtles have individual state and a set of primitive operations available, including rotating and moving. The simulator has turtles which represent the geolocated Pokémons and PokéStops. These, however, do not move, and the Pokémon are spawned only for a period of time. Other turtles represent the players, which are assigned randomly to one of the three teams in the Pokémon Go game: Valor, Mystic, and Instinct; players move around to visit the PokéStops and to capture Pokémons. Simulation parameters include the initial number of Pokémons, the number of PokéStops, the number of players, and the maximum number of Pokémons a player can keep in its storage.

During a simulation, if a player runs out of balls, it moves toward the closest PokéStop and collects a random number of balls from the PokéStop when arriving there. Otherwise, the player chooses a Pokémon as a target, moves toward that Pokémon, and tries to capture



it by “throwing” a ball at it. However, if the player’s Pokémon storage is full, it first has to dispose of one of the Pokémon in storage before attempting a throw. A random number less than 3,500 is generated in each throw: if it is larger than the Pokémon’s strength, the Pokémon is “captured”, then put into the player’s storage, and removed from the simulation. After each throw, successful or otherwise, the ball is “consumed” and the player has one less. During each simulation, we record game activities (collecting balls, capturing and disposing of Pokémon) as provenance data.

We introduce into the simulation different strategies for each team on how its players choose a Pokémon to **target** and to **dispose** of when they need to. Players of the **Valor** team always target for the *strongest* Pokémon, the **Mystic** team the *weakest*, and the **Instinct** team the *closest*. These team-specific targeting behaviours can be switched on/off in the simulation via a button on the interface; when this is off, all players target the closest Pokémon to them. When space is needed in the Pokémon storage, players of the **Instinct** team dispose of the *weakest* Pokémon, the **Mystic** team the *earliest captured*, while the **Valor** team never disposes of a Pokémon and keeps all those captured.

We run two sets of 40 Pokémon Go simulations, with 30 players in each simulation. In the first set, each team follows their individual *targeting* strategy while do not dispose of any Pokémon; in the second, all the teams target the closest Pokémon while following their individual *disposal* strategy above. From the two simulation sets, we have two sets of 1,200 provenance graphs; we call the first PG-T and the second PG-D. Each of those graphs details the in-game actions taken by a particular (simulated) player and is labelled with the player’s team name.

## 4.2 Methodology

For each classification task, in order to ensure the robust evaluation of provenance kernels’ performance compared to that of existing graph kernels and the PNA method, we carry out the following: balancing the input data set (if unbalanced), training classifiers with provenance kernels (PK), generic graph kernels, and provenance network metrics, measuring the performance of each classifier, and comparing their performance. An overview of the full evaluation pipeline, implemented in Python, is depicted in Fig. 4.

**Data balancing** The MIMIC and CollabMap data sets are significantly skewed, being originated from real-world human activities. Therefore, for those data sets, we balance the number of samples in each class by selecting all the samples in the minority class and randomly under-sampling the majority class to produce a balanced data set. Table 3 shows the number of samples used in each classification task after balancing.

**Classification methods** In addition to building classifiers for a classification task in question from the provenance kernels proposed in this paper, we also build classifiers using existing graph kernels, implemented in the Grakel library by Siglidis et al. (2020), and the provenance network metrics as proposed in the PNA method (Huynh et al., 2018).

- **Provenance Kernels:** A provenance kernel is built on provenance types of depth up to a specified level  $h$  which may include (1) *only* the PROV generic (application-agnostic) types, i.e. *ent*, *act*, and *ag*, or (2) application-specific types (such as the `mimic:Patient` and `mimic:Ward` types shown in Fig. 1) *in addition to* the PROV generic types. We

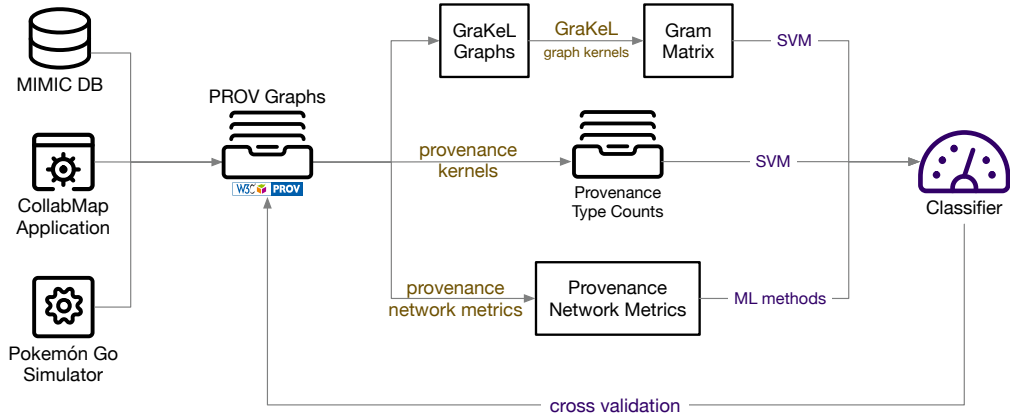


Figure 4: Overview of the evaluation pipeline. Six labelled provenance data sets from three applications are used to build classifiers using provenance kernels, generic graph kernels (provided by the GraKeL library), and provenance network metrics (PNA). Repeated 10-fold cross-validation is carried out to measure the classification accuracy of each method. We also measure the time each method takes to produce provenance kernels, graph kernels, and provenance network metrics (i.e. the yellow step).

test both provenance kernels using only generic types and those including application types in our evaluation; we call the former group PK-G and the latter PK-A. We also evaluate provenance kernels for different levels of  $h$ , from 0 to 5. Hence, the methods we test in these two groups are: G0, G1, ..., G5, A0, ..., A5; the first letter in their names denotes whether they use only PROV generic types (G) or not (A) and the second denotes the specified level  $h$ ; twelve PK-based methods are tested in total.

- **Graph Kernels:** The graph kernels we test are Shortest Path (SP) (Borgwardt and Krieger, 2005), Vertex Histogram (VH) (Sugiyama and Borgwardt, 2015), Edge Histogram (EH) (Sugiyama and Borgwardt, 2015), Graphlet Sampling (GS) (Shervashidze et al., 2009), Weisfeiler-Lehman (WL) (Shervashidze et al., 2011), Hadamard Code (HC) (Kataoka and Inokuchi, 2016), Neighborhood Hash (NH) (Hido and Kashima, 2009), Neighborhood Subgraph Pairwise Distance (NSPD) (Costa and De Grave, 2010).<sup>3</sup> Similar to provenance kernels, Weisfeiler-Lehman and Hadamard Code kernels can be computed up to a specified level  $h$ ; we test those kernels with  $h \in [1, 5]$ . Hence, a total of 16 graph kernels are tested. As shown in Fig. 4, support-vector machines (SVM) are used to build classifiers from both provenance kernels and generic graph kernels. Among the tested graph kernels, the SP, GS, NH, and NSPD kernels take a significantly longer time to run compared to the rest. We, therefore, for comparison purposes, put these methods in a group called GK-slow and the remaining kernels in GK-fast.

3. We have also tried the other graph kernels provided by the Grakel library. However, they either timed out or produced errors when processing graphs in our data sets and, hence, we could not include them in our evaluation.

Table 3: The classification tasks, the number of samples picked from each data set, and the number of application types present in each data set (in addition to PROV generic types).

Data set:	MIMIC	CM-B	CM-R	CM-RS	PG-T	PG-D
Classification labels:	0/1	trusted/uncertain			Valor/Mystic/Instinct	
Random baseline:	50%	50%			33%	
Sample size:	4,586	1,368	2,178	3,382	1,200	1,200
No. application types:	120	8			8	

- **Provenance Network Analytics:** The PNA method proposes calculating 22 network metrics for each provenance graph and using those as the feature vector for that graph. Such feature vectors can be readily taken as inputs by a variety of ML algorithms. Since we are uncertain which algorithm works best with provenance network metrics, we test the following classification algorithms over the metrics: Decision Tree (DT), Random Forest (RF), K-Neighbour (KN), Gaussian Naive Bayes (NB), Multi-layer Perceptron neural network (NN), and Support Vector Machines (SVM). Hence, six methods are tested in total, all are implementations by the Scikit-learn library (Pedregosa et al., 2011) using its default parameters for them. This group of classifiers, which rely on provenance network metrics, is called PNA.

**Performance metrics** The performance of each method is measured by its accuracy in predicting the correct label of a provenance graph (i.e. the number of correct prediction over the total number of samples), which is provided with the above data sets. We use the 10-fold cross-validation procedure to robustly measure the performance. In particular, with all the available provenance traces randomly split into 10 equal subsets, we perform 10 rounds of learning; on each round, a  $1/10$  subset is held out as the test set and the remaining are used as training data. This process is repeated 10 times; hence, we collect 100 measures of accuracy per experiment for each method. In addition, to understand the computation cost of each method, we measure the time it takes to produce provenance kernels, graph kernels, and provenance network metrics (the yellow step in Fig. 4) given the same data set used in a classification task. The recorded time measurements do not include the time taken in training the classifiers nor the time preparing the input GraKeL graphs.

**Comparing performance** Due to the large number of methods evaluated from the five groups (i.e. PK-G, PK-A, GK-slow, GK-fast, PNA), we pick only one best-performing method from each group, i.e. the one with the highest mean classification accuracy within its group. We then compare the mean accuracy of the best-performing PK-based methods (i.e. PK-G, PK-A) against those from the remaining three groups to establish whether PK-based methods offer improved accuracy in the six classification tasks over existing graph kernel and PNA methods. In order to ensure that our comparison results are statistically significant, we carry out the Wilcoxon–Mann–Whitney ranks test (DeGroot and Schervish, 2012, Ch. 10), also known as the Wilcoxon rank-sum test, when comparing the accuracy measurements of two methods. If the test produces a  $p$ -value that is less than 0.05, we reject the null hypothesis that states that the accuracy measurements are from the same distribution,

Table 4: Within each data set, we report the time cost of the best-performing method (shown in parentheses) from each comparison group relative to the time taken by the best-performing PK method (whose time cost shown as 1.0).

	PK-G	PK-A	GK-fast	GK-slow	PNA
MIMIC	1.0 (G5)	1.0 (A4)	1.0 (HC5)	58.1 (GS)	184.9 (SVM)
CM-B	1.0 (G3)	0.8 (A1)	1.2 (HC5)	15.9 (NSPD)	237.9 (DT)
CM-R	0.9 (G0)	1.0 (A0)	1.5 (WL5)	54.7 (NH)	414.2 (RF)
CM-RS	1.0 (G3)	1.0 (A2)	1.2 (WL5)	50.0 (NH)	313.9 (RF)
PG-T	1.0 (G4)	1.0 (A3)	0.7 (WL5)	16.1 (NH)	216.3 (DT)
PG-D	1.5 (G5)	1.0 (A2)	0.7 (WL5)	15.3 (NH)	405.9 (SVM)

i.e one method performs statistically better than the other. Otherwise, both methods are considered to have a similar level of performance.

### 4.3 Evaluation Results

In this section, we report the performance of provenance kernels (PK-G and PK-A) compared to that of existing generic graph kernels (GK-slow and GK-fast) and the PNA method (PNA) across the classification tasks corresponding to the six provenance data sets (MIMIC, CM-B, CM-R, CM-RS, PG-T, and PG-D). As previously mentioned, for brevity, we only report the best-performing method in each group in terms of their mean classification accuracy.

**Computational costs** Before delving into the performance of the five comparison groups, it is pertinent to have an idea of the time costs incurred by them. Within each classification task, using the time cost of the best-performing provenance kernel as the time unit (i.e. 1.0), Table 4 shows the relative time costs of the best-performing method from each comparison group as multiples of the chosen time unit.

Formally, let  $X \in \{\text{PK-G, PK-A, GK-fast, GK-slow, PNA}\}$ . The entry for a given data set associated to the comparison group  $X$  is given by  $(\text{time-of-best-in-}X)/(\text{time-of-best-in-PK})$ , where ‘time-of-best-in- $X$ ’ stands for the time cost of the most accurate method in  $X$ , whereas ‘time-of-best-in-PK’ stands for the time taken by the most accurate method in  $\text{PK} \in \{\text{PK-G, PK-A}\}$ .

We also plot those time costs in Fig. 5 using the logarithmic scale to highlight their differences. Across the data sets, the PK-G and PK-A methods take somewhat a similar time to produce the provenance kernels from the same set of provenance graphs. Their differences are mainly due to the different  $h$  levels (of type propagation). We observe more variation in relative time costs of the GK-fast group’s methods, but they stay in the same magnitude of scale. With the exception of the PG-T data set, the best-performing graph kernels in the GK-slow group, however, take between 15x to 58x longer than the baseline PK method to compute. The PNA methods are the slowest, taking 185x to 400x longer (to compute the provenance network metrics for the same set of provenance graphs). Understanding the computational cost of each method, in addition to its classification performance, will be useful when deciding whether it is suitable for a given classification task.

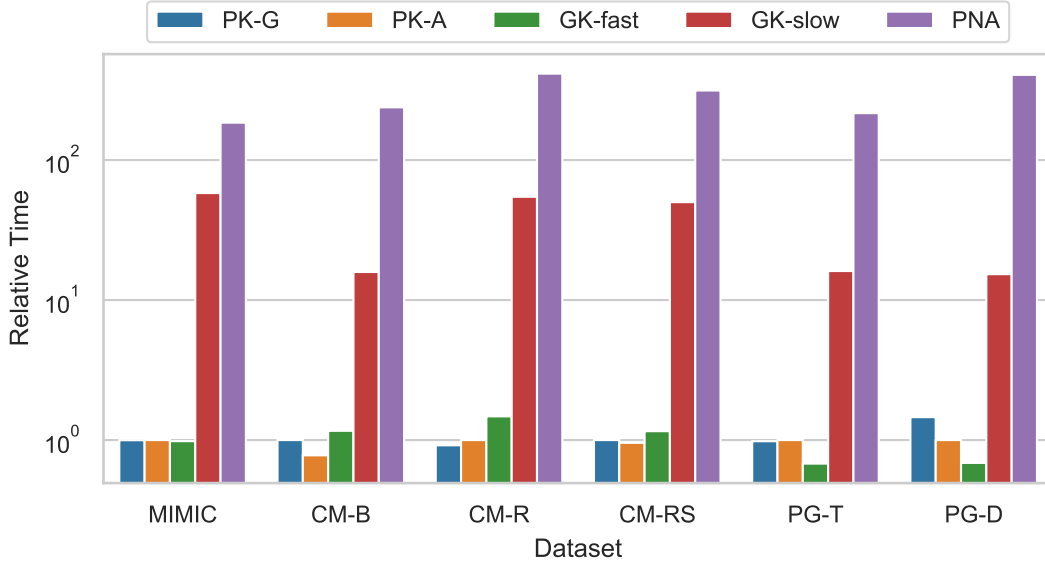


Figure 5: The relative time costs of the best-performing methods reported in Table 4 plotted on the log scale.

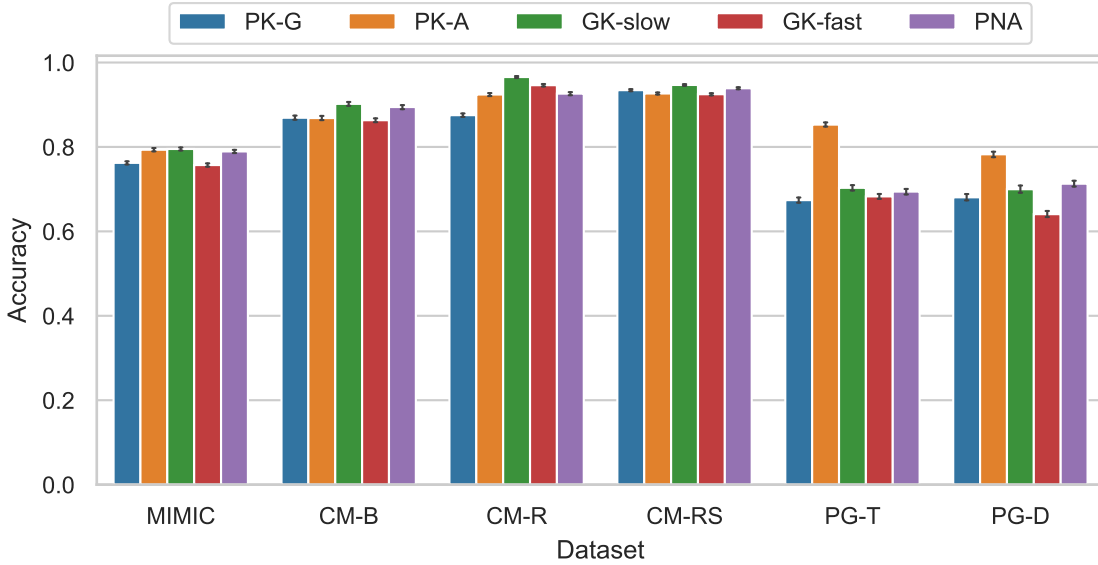


Figure 6: The mean classification accuracy of the best-performing provenance kernels, generic graph kernels, and PNA methods across the six classification tasks. The error bars show the 95-percent confidence intervals.

Table 5: Summary of the accuracy differences between the best-performing PK-based method and the best-performing method in the GK-slow, GK-fast, and PNA groups. An “=” sign means the accuracy difference is not statistically significant; while a positive/negative value shows how much the PK-based method outperforms/under-performs the corresponding GK/PNA method, respectively, when the difference is statistically significant.

Data set:	MIMIC	CM-B	CM-R	CM-RS	PG-T	PG-D
GK-slow	=	-3.3%	-4.1%	-1.2%	+15%	+8.3%
GK-fast	+3.6%	=	-2.2%	+1.0%	+17%	+14%
PNA	=	-2.5%	=	-0.4%	+16%	+7.0%

**Classification accuracy** Fig. 6 plots the mean accuracy of the best-performing provenance kernels compared against that of the best-performing graph kernels and the best-performing PNA methods in the six classification tasks.<sup>4</sup> At first glance, in each task, the accuracy levels attained by the five comparison groups are broadly close and significantly above the random baseline. This shows that the proposed provenance types employed by PK-based methods, the graph information relied on by GK methods, and the provenance network metrics used in PNA methods can all serve effectively as predictors for these classification tasks. However, their contributions to the accuracy of the corresponding classifiers vary. To account for statistical variations, we carry out the Wilcoxon–Mann–Whitney ranks tests to compare the accuracy level of the best PK-based method with that of another comparison group in each classification task. Table 5 presents the results of those tests where an “=” sign indicates that the difference in accuracy, if any, is not statistically significant; otherwise, a positive/negative value represents the accuracy gain/loss attained by the best PK-based method compared to the best method from the corresponding comparison group.

**Comparison with Graph Kernels** If computational/time cost is not a consideration, we find that the GK-slow group generally outperforms the GK-fast group (see green bars vs. red bars in Fig. 6). Compared to the GK-slow group, PK-based methods, however, yield similar levels of accuracy in the MIMIC, outperform in the PG-T and the PG-D task (+15% and +8.3%), and are slightly worse in CollabMap tasks (-3.3%, -4.1%, -1.2%). In terms of computation costs, it should be noted that the best GK-slow methods take 14x to 58x more time<sup>5</sup> than their PK-based counterparts (see Table 4). Compared to the GK-fast group, Table 5 shows that PK-based methods are more accurate in four out of six classification tasks, perform similar in one (CM-B) and worse in only one task (CM-R, -2.2%). Hence, under time constraints (that disqualifies graph kernels in the GK-slow group), the proposed provenance kernels overall outperform the tested graph kernels.

**Comparison with PNA methods** We also report in Table 5 the accuracy differences between the best PK-based methods compared to their PNA counterparts across the six classification tasks. It shows that PK-based methods outperform in two tasks (PG-T: +16%; PG-D: +7%), yield comparable levels of accuracy in another two (MIMIC, CM-R), and are

4. See Table 4 for the identifier of the best-performing method in each group (shown there in parentheses).

5. On our test machine, for instance, the best-performing GK-slow method (Graphlet Sampling) took over 10 minutes to process 4,586 MIMIC graphs while the PK-based counterpart (A4) took 10 seconds.

less accurate in two (CM-B, -2.5%; CM-RS, -0.4%). However, given the significant penalty in computation cost incurred by PNA methods in calculating network metrics (185–400 times, see Table 4) and the small accuracy improvements (in two tasks out of six tested), PK-based methods prove to be better candidates for analysing provenance graphs. Moreover, the PNA method, in some of the tested tasks, employs obscure metrics like the average clustering coefficients predominantly in the trained decision models, making it a challenge to understand why certain classification is decided, even with an interpretable model such as a decision tree classifier. In the following section, we show how provenance types used by the proposed provenance kernels can afford us better interpretability with respect to classification tasks compared to the network metrics employed by PNA methods.

## 5. Explainability

In our evaluation of provenance kernels in Section 4, we used Support Vector Machines to learn from the kernels’ feature vectors and perform classification tasks. This allowed us to fairly compare our model with other graph kernels, also employing SVMs, with regards to accuracy of classification. Techniques such as SVMs, however, are known as black-box models when considering their ability to provide explanations of their predictions. In this section, we show that provenance kernels are compatible with white-box models, and illustrate how they can help improve the explainability of classification models based on them.

The need for interpretable models arises from the need to understand or justify why a certain prediction was made (Freitas, 2014; Doshi-Velez and Kim, 2017). Applications such as medical diagnosis and credit scoring, for example, illustrate why the need for an explanation in addition to the prediction alone is of key importance.

Although provenance types alone do not explain the entirety of a process, they provide practitioners with a tool to better understand the decision process of a classifier. We formalise the steps to explain decision processes using provenance kernels as follows.

- E1 Types Identification:** Provenance kernel is an explicit graph kernel, i.e., we are able to inspect the feature vector used in the classification of each given graph. This, in turn, provides us with the set of provenance types that were used in such predictions.
- E2 Narrative:** As discussed in Section 2, provenance types give us a sequential narrative, which can be associated with real-world events or set of events.
- E3 Extensibility:** The sequential narrative of provenance types can make use of the definition of an extension of a type in Section 2.5. The explanation associated with types of a lower level can serve as a building block to describe longer chains of transformations.
- E4 Instance Retrievalability:** Once provenance types of interest are identified as being associated with a certain prediction, we are able to move our attention away from the types and back to the original graphs. We can do this by retrieving graph instances associated with a given provenance type. This may give us further insights into why a prediction was made as well as flagging other provenance graphs that share such patterns.

We illustrate the main principles discussed above by using a white-box model trained on provenance types from the MIMIC data set. For this purpose, we employ the decision tree classifier from the scikit-learn library using feature vectors of provenance types up to level 2 including application-specific node labels. We select a balanced data set from MIMIC and randomly split it into train and test set (at the ratio 7:3). The tree produced by it is reproduced<sup>6</sup> in Fig. 7. Evaluated over the test set, the trained classifier shows a similar level of accuracy (0.792) compared to our cross-validated results using SVMs (0.793) in Section 4.

Each node of the tree in Fig. 7 is labelled with a number 1 to 7. In non-leaf nodes (1, 2, and 3), a decision rule is applied to each input graph. The number of occurrences of a given type is denoted  $FAx\_y$ , where  $x$  is the type’s depth, and  $y$  is simply an identifier (**E1**). Note that  $FAx\_y$  are therefore non-negative integers. Also,  $x \leq 2$  since we are considering vectors in the context of types which depth is up to 2. If the number of occurrences of the type in question satisfies its corresponding test, then the node on the left-hand side is to be inspected (arrow labelled ‘true’), otherwise the node on the right-hand side is considered. The percentage indicators in each node reflect the proportion of graphs classified as associated with in-hospital fatality (class 1). The higher (resp. lower) the value, the redder (resp. blue) the node’s colour.

Table 6 provides us with the type definitions associated with each one of the counters  $FA2\_2$ ,  $FA0\_26$ ,  $FA0\_9$  used in the decision tree. Their definitions allow us to describe them according to the events they encode.

Starting with node 1, we can infer that the root node of patterns associated with  $FA2\_2$  is an entity, most likely representing a patient. Thus, we may loosely describe this type as representing ‘a patient after being treated in the Intensive Care Unit’ (**E2**, **E3**). Further, from Fig. 7, we can see that one or more occurrences of this type (i.e., the test ‘ $FA2\_2 < 1$ ’ is ‘false’) is associated to a higher concentration of graphs associated with in-hospital mortality (71%, node 3). On the other hand, if  $FA2\_2 = 0$ , i.e.,  $FA2\_2 < 1$  then the number of in-hospital fatalities is down to 20% among the remaining cases (node 2).

Inspecting now node 2, we find that  $FA0\_26$  represents the specific process of intubating a patient, i.e., the patient undertaking an ‘Invasive Ventilation’ procedure (**E2**). Recall that this is a subset of graphs in which  $FA2\_2 = 0$ , i.e., the patient has not necessarily been admitted to the Intensive Care Unit (**E3**). In these cases, if no intubation has been performed ( $FA0\_26 = 0$ ), the concentration of in-hospital fatalities is higher, 34% (node 4) when compared to when the procedure ‘Invasive Ventilation’ is undertaken at least once, 12% (node 5). Finally, we move our attention to node 3 and  $FA0\_9$ , which represents the number of treatments while in intensive care (**E2**). Note that from  $FA2\_2 \geq 1$  (test in node 1 is false) we can infer that  $FA0\_9$  is at least 1. Whether it is exactly 1 or not has an impact on the concentration of hospital-fatality cases. The more treatments (node 7), the smaller the proportion of fatality cases when compared to exactly one treatment (node 6). Finally, note that  $FA2\_2$  can be seen as an extension of  $FA0\_9$  according to the definition in Section 2.5 (**E3**).

---

6. The structure of tree in Fig. 7 is simplified for presentation purposes. The original decision tree and the process of simplifying it is presented and described at <https://github.com/trungdong/provenance-kernel-evaluation>.



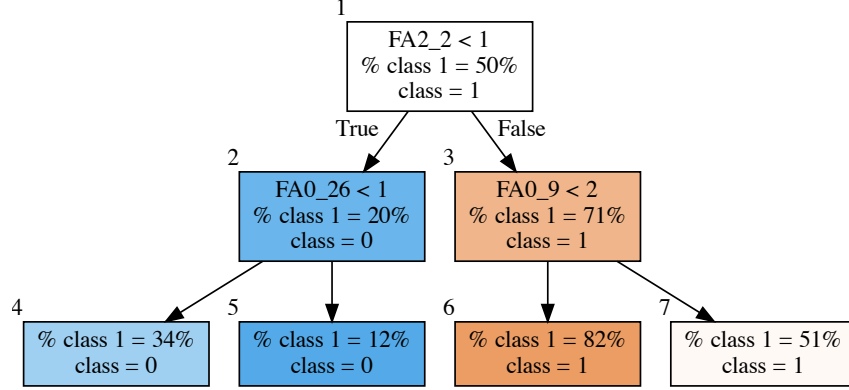


Figure 7: The simplified decision tree produced by scikit-learn’s decision tree classifier over the MIMIC data set using its feature vectors generated from provenance types up to depth 2. Class 1 is associated with in-hospital fatality. The provenance types associated with the features tested in the decision rules of nodes 1, 2, and 3 are defined in Table 6.

Table 6: The provenance types referred by the parameters FA2.2, FA0.26, FA0.9 in Fig. 7. The prefix *m:* indicates an application-specific label from the MIMIC domain, *m:process-225792* refers to an ‘Invasive Ventilation’ procedure.

Parameter	Provenance type represented
FA2.2	( $\{der, gen\}, \{der, gen, use, waw\},$ $\{act, ag, ent, m:IntensiveCare, m:Patient, m:Treating, m:Ward\}$ )
FA0.26	( $\{act, m:Performing, m:process-225792\}$ )
FA0.9	( $\{act, m:IntensiveCare, m:Treating\}$ )

From the discussion above, we may be interested in finding actual graph instances that are represented by the three types in Table 6 (E4). That would provide us with concrete instances, as well as their context, to confirm the narratives we constructed above, i.e., that (1) FA2\_2 is associated to ‘a patient after being treated in the Intensive Care Unit’; (2) FA0\_26 to an ‘Invasive Ventilation’ procedure; and (3) FA0\_9 is associated to ‘treatment while in intensive care’. In order to retrieve instances in which such types are present, we make use of the output of Algorithm in Fig. 2 by querying whether or not a given type of interest is present in a given provenance graph.

## 6. Conclusions and Future Work

With the growing adoption of provenance in a wide range of application domains, the efficient processing and classification of provenance graphs have become imperative. To that end, we introduced a novel graph kernel method tailored for provenance data. Provenance kernels make use of provenance types, which are an abstraction of a node’s neighbourhood taking into account edges and nodes at different distances from it. A provenance type is associated with each node for each depth value  $h$ . A vector is then produced for each graph: it counts the number of occurrences of each (non-empty) provenance type associated to nodes in this graph up to a given depth  $h$ . These feature vectors are then used with standard machine learning algorithms, such as SVMs and decision trees, as shown in the previous two sections. The computational complexity of producing feature vectors for a family of graphs with a total of  $M$  edges is bounded by  $\mathcal{O}(h^2M)$ . Note that the provenance kernel method is applicable to graphs in any domain as long as both edges and nodes are categorically labelled.

In Section 4, we compared provenance kernels against state-of-the-art graph kernels and the PNA method in supervised learning tasks with six data sets of provenance graphs. We showed that provenance kernels are among the fastest methods and, among those, they show high, if not the highest, classification accuracies in the three applications we investigated. An important benefit brought about by provenance types is that they can be used with a white-box model as shown in Section 5 to help us understand better how certain classification is made by the model. We provided a sequence of steps to extract explanations from classifications tasks in white-box models using provenance kernels, making use of the fact that provenance types capture narratives from sequential events in provenance graphs. We thus show how provenance kernels and types may give us further insights into why a particular graph was classified in a particular way.

A given provenance type, when considering only PROV generic node labels, may re-appear in provenance graphs recorded from different applications. The extent of how many types overlap across application domains is an open question. In line with what has been proposed by Kohan Marzagão et al. (2020), an interesting line of future work is to create a library of types across different domains and investigate whether there is a correlation between the high occurrence of certain provenance types and the role they play in classification tasks. Finally, the metric defined in Section 2.5 can be used to compute the Wasserstein distance as originally proposed by Togninalli et al. (2019) before the classification task takes place. In their work, sequences of  $h + 1$  categorical node labels, one per level, similar to what we here define as  $h$ -types, are compared between two nodes to yield a distance measure

which only depends on how many common labels these two nodes share. With provenance types, however, we are able to provide a much more fine-grained metric as proposed in Section 2.5. If results in Togninalli et al. (2019) can be transferred to provenance kernels, we may even further improve their classification performance.

## Acknowledgments

This work was supported by the US Department of Navy award (N62909-18-1-2079) issued by the Office of Naval Research Global and by the UK Engineering and Physical Sciences Research Council (EPSRC Grant EP/S027238/1 for the PLEAD project). The United States Government has a royalty-free license throughout the world in all copyrightable material contained herein.

## Data statement

The data used for the production of this article, along with the associated experiment code, is publicly available at <https://github.com/trungdong/provenance-kernel-evaluation>.

## References

- P. Alper, K. Belhajjame, C. A. Goble, and P. Karagoz. Enhancing and abstracting scientific workflow provenance for data publishing. In *Proceedings of the Joint EDBT/ICDT 2013 Workshops*, pages 313–318, New York, NY, USA, 2013. ACM. ISBN 978-1-4503-1599-9. doi: 10.1145/2457317.2457370.
- A. Berlinet and C. Thomas-Agnan. *Reproducing Kernel Hilbert Spaces in Probability and Statistics*. Springer, Boston, MA, 2011. doi: 10.1007/978-1-4419-9096-9.
- K. M. Borgwardt and H.-P. Kriegel. Shortest-path kernels on graphs. In *Proceedings. Fifth IEEE International Conference on Data Mining*, pages 74–81, Los Alamitos, CA, USA, nov 2005. IEEE Computer Society. doi: 10.1109/ICDM.2005.132. URL <https://doi.ieeecomputersociety.org/10.1109/ICDM.2005.132>.
- F. Chirigati, D. Shasha, and J. Freire. Reprozip: Using provenance to support computational reproducibility. In *Proceedings of the 5th USENIX Conference on Theory and Practice of Provenance*, Berkeley, CA, USA, 2013. USENIX Association.
- F. Costa and K. De Grave. Fast neighborhood subgraph pairwise distance kernel. In *Proceedings of the 27th International Conference on International Conference on Machine Learning, ICML’10*, pages 255–262, Madison, WI, USA, 2010. Omnipress. ISBN 9781605589077.
- G. K. D. de Vries. A fast approximation of the Weisfeiler-Lehman graph kernel for RDF data. In H. Blockeel, K. Kersting, S. Nijssen, and F. Železný, editors, *Machine Learning and Knowledge Discovery in Databases*, pages 606–621, Berlin, Heidelberg, 2013. Springer Berlin Heidelberg. ISBN 978-3-642-40988-2. doi: 10.1007/978-3-642-40988-2\_39.

- G. K. D. De Vries and S. De Rooij. Substructure counting graph kernels for machine learning from rdf data. *Journal of Web Semantics*, 35:71–84, 2015.
- M. H. DeGroot and M. J. Schervish. *Probability and Statistics*. Pearson, 4 edition, 2012. ISBN 978-0321500465.
- F. Doshi-Velez and B. Kim. Towards A Rigorous Science of Interpretable Machine Learning. *arXiv e-prints*, art. arXiv:1702.08608, Feb 2017.
- A. Feragen, N. Kasenburg, J. Petersen, M. de Bruijne, and K. Borgwardt. Scalable kernels for graphs with continuous attributes. In *Advances in neural information processing systems*, pages 216–224, 2013.
- A. A. Freitas. Comprehensible classification models: A position paper. *SIGKDD Explor. Newsl.*, 15(1):1–10, Mar. 2014. ISSN 1931-0145. doi: 10.1145/2594473.2594475. URL <http://doi.acm.org/10.1145/2594473.2594475>.
- T. Gärtner, P. Flach, and S. Wrobel. On graph kernels: Hardness results and efficient alternatives. In *Learning theory and kernel machines*, pages 129–143. Springer, 2003.
- A. Grover and J. Leskovec. Node2vec: Scalable feature learning for networks. In *Proceedings of the 22nd ACM SIGKDD International Conference on Knowledge Discovery and Data Mining*, KDD ’16, page 855–864, New York, NY, USA, 2016. Association for Computing Machinery. ISBN 9781450342322. doi: 10.1145/2939672.2939754. URL <https://doi.org/10.1145/2939672.2939754>.
- S. Hido and H. Kashima. A linear-time graph kernel. In *Proceedings of the 2009 Ninth IEEE International Conference on Data Mining*, ICDM ’09, page 179–188, Los Alamitos, CA, USA, dec 2009. IEEE Computer Society. ISBN 9780769538952. doi: 10.1109/ICDM.2009.30.
- T. D. Huynh, M. Ebden, J. Fischer, S. Roberts, and L. Moreau. Provenance Network Analytics. *Data Mining and Knowledge Discovery*, feb 2018. ISSN 1384-5810. doi: 10.1007/s10618-017-0549-3. URL <http://link.springer.com/10.1007/s10618-017-0549-3>.
- A. E. W. Johnson, T. J. Pollard, L. Shen, L.-w. H. Lehman, M. Feng, M. Ghassemi, B. Moody, P. Szolovits, L. Anthony Celi, and R. G. Mark. MIMIC-III, a freely accessible critical care database. *Scientific Data*, 3(1):160035, 2016. doi: 10.1038/sdata.2016.35.
- G. Kalna and D. J. Higham. Clustering coefficients for weighted networks. In *Symposium on network analysis in natural sciences and engineering*, page 45, 2006.
- T. Kataoka and A. Inokuchi. Hadamard code graph kernels for classifying graphs. In *Proceedings of the 5th International Conference on Pattern Recognition Applications and Methods - Volume 1: ICPRAM*, pages 24–32. INSTICC, SciTePress, 2016. ISBN 978-989-758-173-1. doi: 10.5220/0005634700240032.
- D. Kohan Marzagão, T. Huynh, and L. Moreau. Incremental inference of provenance types. In *8th International Provenance and Annotation Workshop (IPAW’20) - Forthcoming*, 2020.

- N. M. Kriege, F. D. Johansson, and C. Morris. A survey on graph kernels. *Applied Network Science*, 5(1):1–42, 2020. doi: 10.1007/s41109-019-0195-3.
- U. Lösch, S. Bloehdorn, and A. Rettinger. Graph kernels for rdf data. In E. Simperl, P. Cimiano, A. Polleres, O. Corcho, and V. Presutti, editors, *The Semantic Web: Research and Applications*, pages 134–148, Berlin, Heidelberg, 2012. Springer Berlin Heidelberg. ISBN 978-3-642-30284-8.
- X. Ma, P. Fox, C. Tilmes, K. Jacobs, and A. Waple. Capturing provenance of global change information. *Nature Climate Change*, 4(6):409–413, 2014. ISSN 1758-678X. doi: 10.1038/nclimate2141.
- L. Moreau. Aggregation by provenance types: A technique for summarising provenance graphs. In *Graphs as Models 2015 (An ETAPS’15 workshop)*, pages 129–144, London, UK, apr 2015. Electronic Proceedings in Theoretical Computer Science. doi: 10.4204/EPTCS.181.9.
- L. Moreau and P. Missier. PROV-DM: The PROV data model. Technical report, World Wide Web Consortium, 2013. URL <http://www.w3.org/TR/2013/REC-prov-dm-20130430/>. W3C Recommendation.
- G. Nikolentzos, G. Siglidis, and M. Vazirgiannis. Graph kernels: A survey. *arXiv preprint arXiv:1904.12218*, 2019.
- J. Paavilainen, H. Korhonen, K. Alha, J. Stenros, E. Koskinen, and F. Mayra. The pokémon go experience: A location-based augmented reality mobile game goes mainstream. In *Proceedings of the 2017 CHI Conference on Human Factors in Computing Systems*, CHI ’17, page 2493–2498, New York, NY, USA, 2017. Association for Computing Machinery. ISBN 9781450346559. doi: 10.1145/3025453.3025871. URL <https://doi.org/10.1145/3025453.3025871>.
- F. Pedregosa, G. Varoquaux, A. Gramfort, V. Michel, B. Thirion, O. Grisel, M. Blondel, P. Prettenhofer, R. Weiss, V. Dubourg, J. Vanderplas, A. Passos, D. Cournapeau, M. Brucher, M. Perrot, and E. Duchesnay. Scikit-learn: Machine learning in Python. *Journal of Machine Learning Research*, 12(85):2825–2830, 2011. URL <http://jmlr.org/papers/v12/pedregosa11a.html>.
- B. Perozzi, R. Al-Rfou, and S. Skiena. Deepwalk: Online learning of social representations. In *Proceedings of the 20th ACM SIGKDD International Conference on Knowledge Discovery and Data Mining*, KDD ’14, page 701–710, New York, NY, USA, 2014. Association for Computing Machinery. ISBN 9781450329569. doi: 10.1145/2623330.2623732. URL <https://doi.org/10.1145/2623330.2623732>.
- N. Pržulj. Biological network comparison using graphlet degree distribution. *Bioinformatics*, 23(2):e177–e183, 2007.
- S. D. Ramchurn, T. D. Huynh, M. Venanzi, and B. Shi. CollabMap: Crowdsourcing maps for emergency planning. In *5th ACM Web Science Conference (WebSci ’13)*, pages 326–335, 2013. doi: 10.1145/2464464.2464508.

- S. D. Ramchurn, T. D. Huynh, F. Wu, Y. Ikuno, J. Flann, L. Moreau, J. E. Fischer, W. Jiang, T. Rodden, E. Simpson, S. Reece, S. Roberts, and N. R. Jennings. A disaster response system based on human-agent collectives. *Journal of Artificial Intelligence Research*, 57:661–708, 2016. doi: 10.1613/jair.5098. URL <http://www.jair.org/papers/paper5098.html>.
- L. F. Ribeiro, P. H. Saverese, and D. R. Figueiredo. Struc2vec: Learning node representations from structural identity. In *Proceedings of the 23rd ACM SIGKDD International Conference on Knowledge Discovery and Data Mining*, KDD '17, page 385–394, New York, NY, USA, 2017. Association for Computing Machinery. ISBN 9781450348874. doi: 10.1145/3097983.3098061. URL <https://doi.org/10.1145/3097983.3098061>.
- P. Ristoski and H. Paulheim. Semantic web in data mining and knowledge discovery: A comprehensive survey. *Journal of Web Semantics*, 36:1–22, 2016. ISSN 1570-8268. doi: 10.1016/j.websem.2016.01.001.
- P. Rosso, D. Yang, and P. Cudré-Mauroux. Beyond triplets: Hyper-relational knowledge graph embedding for link prediction. In *Proceedings of The Web Conference 2020*, WWW '20, page 1885–1896, New York, NY, USA, 2020. Association for Computing Machinery. ISBN 9781450370233. doi: 10.1145/3366423.3380257.
- N. Shervashidze, S. Vishwanathan, T. Petri, K. Mehlhorn, and K. Borgwardt. Efficient graphlet kernels for large graph comparison. volume 5 of *Proceedings of Machine Learning Research*, pages 488–495, Hilton Clearwater Beach Resort, Clearwater Beach, Florida USA, 16–18 Apr 2009. PMLR. URL <http://proceedings.mlr.press/v5/shervashidze09a.html>.
- N. Shervashidze, P. Schweitzer, E. J. v. Leeuwen, K. Mehlhorn, and K. M. Borgwardt. Weisfeiler-Lehman graph kernels. *Journal of Machine Learning Research*, 12(Sep):2539–2561, 2011.
- G. Siglidis, G. Nikolentzos, S. Limnios, C. Giatsidis, K. Skianis, and M. Vazirgianis. GraKeL: A Graph Kernel Library in Python. *Journal of Machine Learning Research*, 21(54):1–5, 2020. URL <http://jmlr.org/papers/volume21/18-370/18-370.pdf>.
- M. Sugiyama and K. Borgwardt. Halting in random walk kernels. In C. Cortes, N. D. Lawrence, D. D. Lee, M. Sugiyama, and R. Garnett, editors, *Advances in Neural Information Processing Systems 28*, pages 1639–1647. Curran Associates, Inc., 2015. URL <https://papers.nips.cc/paper/5688-halting-in-random-walk-kernels>.
- S. Tisue and U. Wilensky. NetLogo: A simple environment for modeling complexity. In *Conference on Complex Systems*, pages 1–10, 2004. URL <http://ccl.sesp.northwestern.edu/papers/netlogo-iccs2004.pdf>.
- M. Togninalli, E. Ghisu, F. Llinares-López, B. Rieck, and K. Borgwardt. Wasserstein Weisfeiler-Lehman graph kernels. In *Advances in Neural Information Processing Systems*, pages 6439–6449, 2019.

- S. V. N. Vishwanathan, N. N. Schraudolph, R. Kondor, and K. M. Borgwardt. Graph kernels. *Journal of Machine Learning Research*, 11(Apr):1201–1242, 2010.
- D. Yang, P. Rosso, B. Li, and P. Cudre-Mauroux. Nodesketch: Highly-efficient graph embeddings via recursive sketching. In *Proceedings of the 25th ACM SIGKDD International Conference on Knowledge Discovery & Data Mining*, KDD '19, page 1162–1172, New York, NY, USA, 2019. Association for Computing Machinery. ISBN 9781450362016. doi: 10.1145/3292500.3330951.